CLINICAL REPORT

AMERICAN JOURNAL OF medical genetics PART A

A Homozygous *B3GAT3* Mutation Causes a Severe Syndrome With Multiple Fractures, Expanding the Phenotype of Linkeropathy Syndromes

Kelly L. Jones,[1] Ulrike Schwarze,[2] Margaret P. Adam,[1] Peter H. Byers,[2,3] and Heather C. Mefford[1]*

[1]Division of Genetic Medicine, Department of Pediatrics, University of Washington & Seattle Children's Hospital, Seattle, Washington

[2]Department of Pathology, University of Washington, Seattle, Washington

[3]Department of Medicine, University of Washington, Seattle, Washington

Manuscript Received: 1 April 2015; Manuscript Accepted: 3 June 2015

Linkeropathies are a group of syndromes characterized by short stature, radio-ulnar synostosis, decreased bone density, congenital contractures and dislocations, joint laxity, broad digits, brachycephaly, small mouth, prominent eyes, short or webbed neck, congenital heart defects and mild developmental delay. Linkeropathies are due to enzymatic defects in the synthesis of the common linker region that joins the core proteins to their glycosaminoglycan (GAG) side chains. The enzyme glucuronyltransferase 1, encoded by *B3GAT3*, adds the last four saccharides comprising the linker region. Mutations in *B3GAT3* have been reported in two unrelated families with the same homozygous mutation (c.830G>A, p.Arg277Gln). We report on a patient with a novel homozygous *B3GAT3* (c.667G>A, p.Gly223Ser) mutation and a history of multiple fractures, blue sclerae, and glaucoma. Our patient was a 12-month-old boy born to consanguineous parents and, like previously reported patients, he had bilateral radio-ulnar synostosis, severe osteopenia, an increased gap between first and second toes, bilateral club feet, and atrial and ventricular septal defects. He had the additional features of bilateral glaucoma, hypertelorism, upturned nose with anteverted nares, a small chest, a diaphragmatic hernia, multiple fractures, arachnodactyly, overlapping fingers with ulnar deviation, lymphedema, hypotonia, hearing loss, and perinatal cerebral infarction with bilateral supra- and infratentorial subdural hematomas. We highlight the extended phenotypic range of *B3GAT3* mutations and a provide comparative overview of the phenotypic features of the linkeropathies associated with mutations in *XYLT1*, *B4GALT7*, *B3GALT6*, and *B3GAT3*.

Key words: linkeropathy; *B3GAT3*; proteoglycan disorder; congenital disorder of glycosylation; multiple fractures

How to Cite this Article:
Jones KL, Schwarze U, Adam MP, Byers PH, Mefford HC. 2015. A homozygous *B3GAT3* mutation causes a severe syndrome with multiple fractures, expanding the phenotype of linkeropathy syndromes.
Am J Med Genet Part A 9999:1–6.

INTRODUCTION

Proteoglycans (PGs) are cell surface molecules and essential components of extracellular matrices regulating cell-cell and cell-matrix interactions, cell proliferation, differentiation and development. PGs are composed of a protein core with variable glycosaminoglycan (GAG) side chains, which are attached to serine residues via a tetrasaccharide linker (Fig. 1). Recently, a group of related disorders due to defects in one of the four steps in synthesis of the common linker region has been described [Nakajima et al., 2013]. These multisystem disorders are referred to as "linkeropathies" [Freeze 2006; Nakajima et al., 2013].

The enzymes involved in the synthesis of the common linker region and their corresponding genes are xylosyltransferases 1 and 2 (*XYLT1* and *XYLT2*), galactosyltransferase 1 (*B4GALT7*) and galactosyltransferase 2 (*B3GALT6*) and glucuronosyltransferase 1 (*B3GAT3*) [Haltiwanger and Lowe 2003; Sugahara et al., 2003; Häcker et al., 2005; Bishop et al., 2007], and bi-allelic mutations in most genes have been reported to cause human disease. Mutations in *XYLT1* cause Desbuquois dysplasia type 2 (OMIM #615777), previously reported in nine patients [Bui et al., 2014; Schreml et al., 2014]. Mutations in *B4GALT7* are associated with the progeroid

*Correspondence to:
Heather C. Mefford, M.D., Ph.D., Division of Genetic Medicine, Department of Pediatrics, University of Washington, RR349A/Box 356320, Seattle, WA 98195.
E-mail: hmefford@uw.edu
Article first published online in Wiley Online Library (wileyonlinelibrary.com): 00 Month 2015
DOI 10.1002/ajmg.a.37209

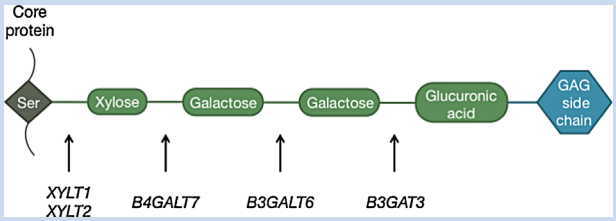

FIG. 1. Diagram of the linkeropathy genes and their associated syndromes. Proteoglycans are highly glycosylated proteins with covalently attached glycosaminoglycan (GAG) chain. The GAG is attached via a tetrasaccharide bridge (indicated by the four green ovals) to a serine (Ser) residue in the core protein. Human disorders previously associated with mutations in each gene are discussed in the text, and specific phenotypic features are shown in Table I.

type of Ehlers–Danlos syndrome (OMIM #130070), previously reported in 26 patients [Kresse et al., 1987; Faiyaz-Ul-Haque et al., 2004; Guo et al., 2013; Cartault et al., 2015]. Mutations in *B3GALT6* are associated with spondyloepimetaphyseal dysplasia with joint laxity, type 1 (OMIM # 271640) reported in 16 patients [Malfait et al., 2013; Nakajima et al., 2013]. A single homozygous mutation in *B3GAT3*, involved in the final step of linker region synthesis, has been reported in six patients with multiple joint dislocations, short stature, craniofacial dysmorphism and congenital heart defects (OMIM #245600) in two families [Baasanjav et al., 2011; von Oettingen et al., 2014].

Here, we describe a patient from a consanguineous family with a novel homozygous *B3GAT3* mutation and a very severe phenotype, expanding the phenotype associated with this disorder. We review the phenotypic features of the linkeropathies associated with mutations in *XYLT1*, *B4GALT7*, *B3GALT6*, and *B3GAT3*.

CLINICAL REPORT

The patient was a 12-month-old Mexican boy born to parents who were second cousins once removed, whose family history was negative for congenital or skeletal anomalies. Routine ultrasound at 19 weeks estimated gestation identified bilateral clubfeet, clenched hands, and increased nuchal translucency. A structural heart defect was noted and initially thought to be a hypoplastic left heart. Cell-free DNA aneuploidy screen was negative.

The infant was delivered vaginally at term and had a birth weight of 2.56 kg (4th centile), length of 44.5 cm (−2.93 SD) and head circumference of 33 cm (11th centile). At birth, the previously identified clubfeet and clenched hands were present along with a large anterior fontanelle, hypertelorism, bilateral glaucoma, short and upturned nose with a flat nasal bridge, anteverted nares, and a short neck with redundant tissue (Fig.2 A–C). His upper extremities had decreased flexion creases on interphalangeal joints, camptodactyly, arachnodactyly, ulnar deviation of fingers with the left 2nd and 3rd fingers overlapping the 4th and 5th (Fig. 2D and E). His lower extremities showed bilateral sandal gaps (Fig. 2F). He also had significant hypotonia and lymphedema.

A skeletal survey revealed diffuse demineralization with bowed humeri, bilateral radio-ulnar synostosis, metaphyseal widening, femur fractures, and clubfeet; no joint dislocations were noted. The survey showed a large anterior fontanelle, 11 pairs of ribs and a small thorax (Fig. 3A, 3C and 3D). The small thorax resulted in restrictive lung disease that required significant respiratory support with upper respiratory infections. At 3 months, our patient began to require supplemental oxygen that ultimately resulted in a 2 months long intubation. He was slowly weaned to minimal respiratory support at night when he developed rhinovirus at age 10 months. This resulted in another intubation and slow respiratory wean. During the first year, the patient has had approximately 25 fractures in all four extremities and vertebrae (Fig. 3E); some fractures were incurred during routine blood pressure monitoring. Pamidronate administration began around six months of age. After two months, zones of calcification with sclerotic metaphyseal bands were evident, consistent with bisphosphonate therapy; however, our patient continued to have fractures after six months of therapy. By 12 months of age, plain films of the patient's abdomen and pelvis showed short ilia with flat acetabular angles (Fig. 3B).

Postnatal echocardiogram revealed that the patient did not have a hypoplastic left heart but rather a large atrial septal defect, ventricular septal defect and a patent ductus arteriosus. At about 3 months of age, brainstem auditory evoked response evaluation showed moderate conductive hearing loss bilaterally. At 6 months of age, trabeculotomy for the patient's bilateral glaucoma was attempted, but discontinued because of uveal prolapse due to marked scleral thinning. A brain MRI at 2 days of age revealed multiple foci of infarction in the left cerebral hemisphere and bilateral supra- and infra-tentorial subdural hematomas overlying the bilateral parietooccipital lobes and bilateral cerebellar hemispheres. A subsequent thrombophilia work up was negative. At 12 months of age, a chest X-ray revealed a Morgagni type diaphragmatic hernia. Development at 9 months showed that our patient was beginning to bat objects and have some brief consonant babbling, but he was unable to roll over or sit independently.

GENETIC TESTING

The genetic evaluation began with analysis of very long chain fatty acids given the large fontanelle, hypotonia and flat nasal bridge; however, this test was negative. Other biochemical testing included a sterol panel and transferrin and apolipoprotein CIII isoform analysis for disorders of glycosylation and these tests were also negative. SNP microarray revealed a 121–201 kb deletion of *PARK2* that was not thought to contribute to the patient's phenotype. In addition, multiple long stretches of homozygosity of at least 3 Mb were noted, which comprised approximately 265 Mb or 13% of the autosomal genome. Because of the significant degree of homozygosity, the possibility of at least one autosomal recessive condition was considered. All OMIM genes with an autosomal recessive phenotype were identified using the Santa Cruz Genome Browser (http://www.genome.ucsc.edu). Consequently, a number of interesting candidate genes were considered, initially focusing on the genes with associated with multiple fractures and radio-ulnar synostosis. *WNT1* (multiple fractures and hypotonia), *B4GALT7*

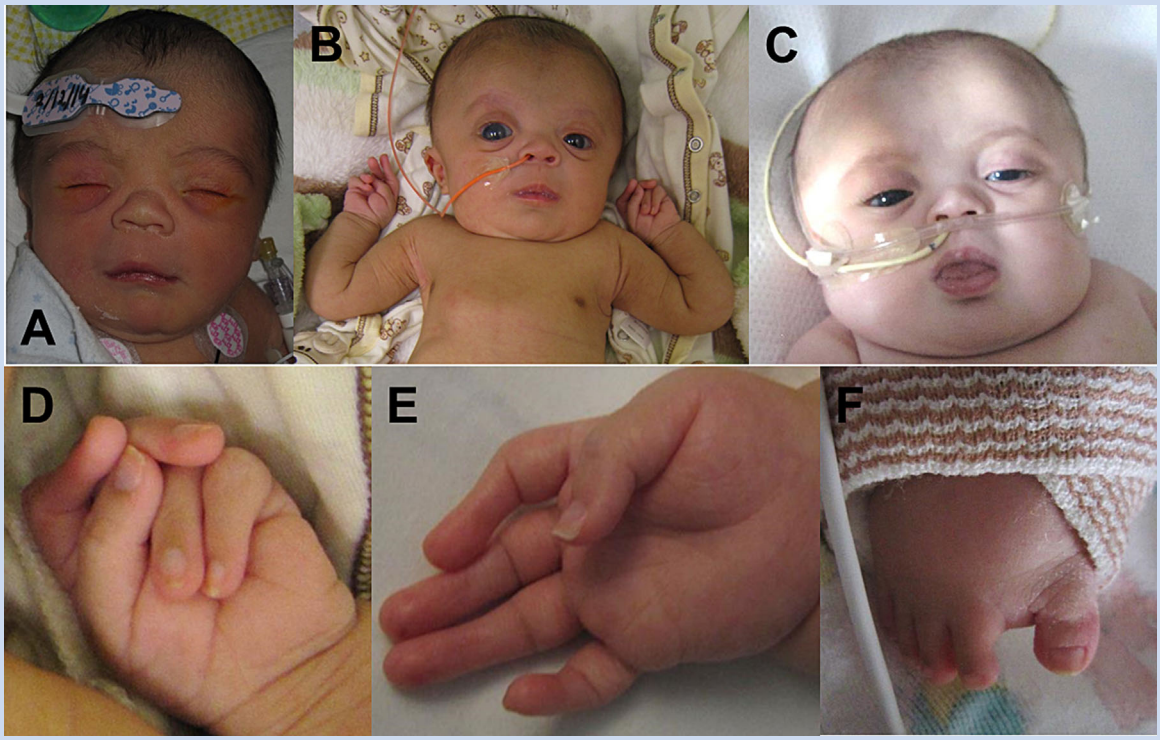

FIG. 2. A-C: Face at 1 day old (A), 2 months (B) and 9 months (C): Prominent forehead, prominent eyes with right greater than left, blue sclerae with corneal clouding, flat nasal bridge with short nose, small mouth, short neck. Feeding tube present at 2 and 9 months and nasal cannula present at 9 months. D: Left hand at 2 months: overlapping digits. E: Right hand at 2 months: Camptodactyly with absent distal flexion creases, broad tips of digits. F: Right foot at 6 months: Sandal gap between 1st and 2nd toes.

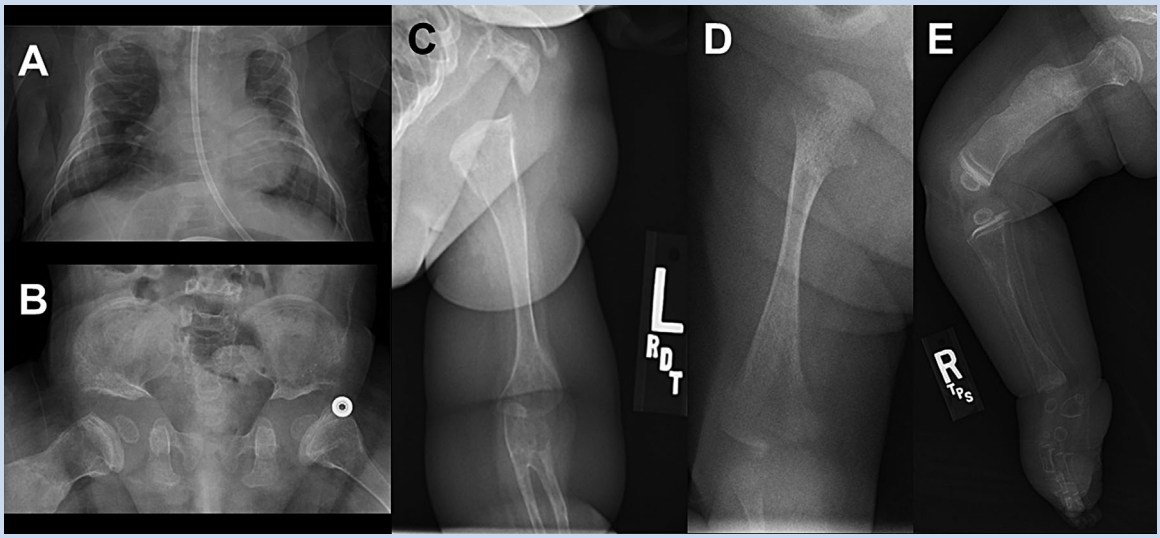

FIG. 3. A: Small chest with nasogastric tube at 3 months of age. B: Small ilia with flat acetabular angles. C: Radio-ulnar synostosis of left arm. D: Right femur at 3 weeks of age with fracture and metaphyseal flaring. E: Right lower extremity at 8 months of age with healing fractures. All five radiographs show bone demineralization.

TABLE I. Comparison of Clinical Features in Patients With Linkeropathies

	XYLT1 (n = 9)	B4GALT7 (n = 26)	B3GALT6 (n = 16)	B3GAT3 (n = 6)	
Feature	**Bui et al. [2014]; Schreml et al. [2014]**	**Kresse et al. [1987]; Faiyaz-Ul-Haque [2004]; Guo et al. [2013]; Cartault et al. [2015]**	**Malfait et al. [2013]; Nakajima et al. [2013]**	**Baasanjav et al. [2011]; von Oettingen et al. [2014]**	**Our patient**
Skeletal abnormalities					
Short stature	9/9 (range: −5.5 to −9 SD)	23/23 (range: −3.5 to −8.8 SD)	13/15 (range: −1.6 to −10.7 SD)	6/6 (<3rd %; −3.43 SD)	Yes (−2.13 SD at 9 months)
Joint laxity	6/6	11/24	10/13	6/6	No
Joint dislocations	6/8	23/23	8/12	6/6	No
Advanced bone age/carpal ossification	5/5	12/16	5/10	0/1	Unknown
Decreased bone density	NR	2/3	2/2	Yes but not specified	Yes
Multiple fractures	NR	0/2	3/4	NR	Yes
Joint contractures	NR	NR	5/14	5/5	Yes
Pectus abnormality	3/3	7/22	4/4	1/1	No
Kyphosis and/or scoliosis	NR	6/22	14/14	0/1	No
Radioulnar synostosis	0/2	13/24	NR	0/1	Yes
Restricted elbow movement	NR	4/4	9/11	1/1	Yes
Broad tips of fingers and/or toes[a]	2/2	4/24	11/15	6/6	Yes
Long fingers and/or toes	NR	4/4	NR	NR	Yes
Iliac abnormalities[b]	1/1	NR	14/14	1/1	Yes
Monkey wrench or Swedish key appearance of femora	6/6*	9/19	NR	NR	No
Metaphyseal abnormalities[c]	NR	3/3	12/13	1/1	Yes
Foot abnormalities[d]	4/4	3/3	8/16	6/6	Yes
Sandal gap between toes	1/1*	1/1*	1/1*	1/1	Yes
Craniofacial features					
Prominent forehead	NR	26/26	9/10	6/6	Yes
Prominent/proptotic eyes	2/2	24/24	8/11	6/6	Yes
Blue sclerae	3/3	NR	4/4	NR	Yes
Hypertelorism	NR	22/22	NR	NR	No
Downslanting palpebral fissures	NR	1/1	2/2	3/5	No
Glaucoma/increased intraocular pressure	0/2	5/21	1/1	NR	Yes
Depressed nasal bridge	1/1	NR	1/1	5/6	Yes
Microstomia	NR	25/25	NR	4/6	Yes
Short and/or webbed neck	1/1	NR	NR	6/6	Yes
Dermatologic abnormalities					
Hyperextensible skin	NR	24/25	8/13	0/1	No
Atrophic scars	NR	2/2	2/2	0/1	Not currently
Other findings					
Developmental delay, learning difficulties, or cognitive deficits	8/9	16/26	6/6	1/6	Yes
Hypotonia	3/3	4/4	9/16	0/1	Yes
Cardiovascular abnormalities	0/2	0/1	0/2	6/6	Yes

NR, not reported.
*Feature was identified from picture.
[a]Includes bifid thumbs, prominent digital pads.
[b]Comprises of short ilia, flattened iliac wings or hypoplastic iliac bodies.
[c]Includes widening, flaring or other unspecified abnormalities.
[d]Includes clubfeet, broad feet, pes planus, talipes equinovarus, metatarsus varus.

(glaucoma and radio-ulnar synostosis in progeroid Ehlers–Danlos syndrome), *B3GALT6* (multiple fractures and spatulate terminal phalanges), and *IFITM5* (multiple fractures with marked density at the epiphyseal–metaphyseal boundaries) sequences were all normal. Sequence analysis of *B3GAT3* revealed a novel homozygous missense mutation p.Gly223Ser, which was located within a 10.55 Mb region of homozygosity. Because our patient's phenotype was more severe than reported in the literature, there was concern that the *B3GAT3* mutation may not explain all his features and that the patient may have an additional autosomal recessive syndrome. Consequently, clinical exome sequence analysis identified the same *B3GAT3* mutation but did not reveal additional causative mutations. Functional studies could not be performed because the family declined further genetic analyses.

DISCUSSION

B3GAT3 encodes the 335 amino acid glucuronosyltransferase I protein that catalyzes the addition of glucuronic acid, the final sugar moiety in the tetrasaccharide linker region [Kitagawa et al., 1998]. A p.Arg277Gln mutation has been reported in two consanguineous families, both from the United Arab Emirates. The first report described five affected siblings [Baasanjav et al., 2011] while the second report described a single affected child [von Oettingen et al., 2014]. Baasanjav et al. [2011] performed functional studies on two siblings with the homozygous p.Arg277Gln mutations and showed that the glucuronosyltransferase I activity was decreased to 3–5% of age-matched control levels. As hypothesized, they showed that the mutation resulted in a partial deficiency of all three O-glycanated proteoglycans (dermatan sulfate, chondroitin sulfate and heparan sulfate) [Baasanjav et al., 2011].

The homozygous p.Gly223Ser mutation has not previously been reported in humans. Review of the ExAC browser (http://exac.broadinstitute.org) revealed that this mutation was present in 1 of 119,290 alleles with a frequency of $8.383e^{-6}$. In contrast, the p.Arg277Gln mutation was present in 3 of 120,974 alleles with a frequency of $2.48e^{-5}$. There were no homozygotes for either mutation. PolyPhen2 [Adzhubei et al., 2010] analysis of the p.Gly223Ser was predicted to be "probably damaging" with a score of 0.935 while the p.Arg277Gln mutation was predicted to be "possibly damaging" with a score of 0.763. The GERP score for the p.Gly223Ser mutation was 3.78 while the p.Arg277Gln mutation was 5.31. Additionally, Gulberti et al. [2005] found that substituting an alanine residue for either Gly222 or Gly223 markedly impaired the glucuronosyltransferase 1 activity of recombinant human glucuronosyltransferase 1 in yeast cells as part of a study investigating the specificity of glycosyltransferases.These analyses bolster the conclusion that both the p.Gly223Ser and the p.Arg277Gln mutations are likely pathogenic.

Our patient has many features present in the six previously reported patients with *B3GAT3* mutations (Table I), including short stature, prominent forehead and eyes, broad fingers and toes, and cardiovascular abnormalities [Baasanjav et al., 2011; von Oettingen et al., 2014]. He has the additional features of blue sclerae, glaucoma, arachnodactyly, hearing loss, multiple fractures, a diaphragmatic hernia and a small thorax. None of these features have been previously reported in an individual with a *B3GAT3* mutation. Even at 12 months of age, it is clear that our patient has a more severe phenotype than reported previously and it is expected that he will have a significantly different clinical course, expanding the phenotypic spectrum associated with *B3GAT3* mutations.

While our patient has features not previously reported in patients with *B3GAT3* mutations, some of these have been reported in other linkeropathies (Table I). For example, multiple fractures and blue sclerae have been reported in patients with *B3GALT6* mutations [Malfait et al., 2013]. Blue sclerae and small chests have also been reported in patients with *XYLT1* mutations [Bui et al., 2014]. While hypotonia has not been reported in individuals with *B3GAT3* mutations, it has been reported in all other linkeropathies. These similarities suggest a phenotypic overlap in individuals who have a deficiency in the biosynthesis of the common linker region [Kresse et al., 1987; Faiyaz-Ul-Haque et al., 2004; Guo et al., 2013; Malfait et al., 2013; Nakajima et al., 2013; Bui et al., 2014].

This conclusion is further supported by the phenotypic features shared among all of the linkeropathies (Fig. 4). These include short stature, prominent forehead and eyes, pectus abnormalities, joint laxity and dislocations, broad fingertips, foot abnormalities, hypotonia, and developmental delays [Kresse et al., 1987; Faiyaz-Ul-Haque et al., 2004; Baasanjav et al., 2011; Guo et al., 2013; Malfait et al., 2013; Nakajima et al., 2013; Bui et al., 2014; Schreml et al., 2014; von Oettingen et al., 2014; Cartault et al., 2015]. Other features are present in some disorders, such as cardiac defects, radio-ulnar synostosis, monkey wrench or Swedish key appearance of the femora, and atrophic scars. This phenotypic disparity may be due to varying levels of gene expression in different tissues as suggested by Nakajima et al. [2013]. Another consideration may be that the linkeropathies have not been fully characterized. Several previous reports focused on a particular aspect of the phenotype, such as the skeletal features, and may not have described other systemic features that were present.

In summary, we describe a severe phenotype caused by a homozygous c.667G>A mutation in *B3GAT3*, resulting in the

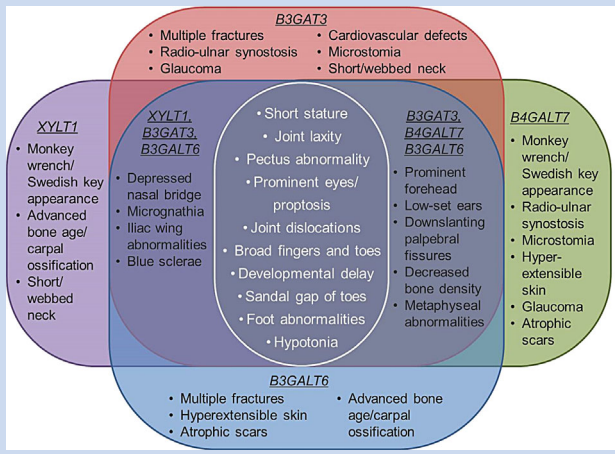

FIG. 4. Diagram of the features shared by all of the linkeropathies along with other common features shared by several of the linkeropathies.

p.Gly223Ser change in glucuronosyltransferase I. This expands the number of syndromes caused by homozygous *B3GAT3* mutations. Based on our experience, we suggest considering *B3GAT3* mutations in a patient with multiple fractures, prominent forehead and eyes, hypotonia and developmental delay, who had a negative evaluation for osteogenesis imperfecta. Furthermore, a clinician should consider the linkeropathies when a patient presents with short stature, prominent forehead and eyes, joint laxity and dislocations, iliac and metaphyseal abnormalities, broad fingertips, foot abnormalities and developmental delay. As additional clinical descriptions of these disorders are reported, further insight will characterize the linkeropathies individually and as a group.

ACKNOWLEDGMENTS

The authors would like to thank the patient and family for their participation. We also would like to thank Anita E. Beck, MD, PhD for her thoughtful and helpful discussions. K.L.J. was supported by NIH/NIGMS training grant 5T32GM007454. This project was supported in part by funds from the Department of Pathology and the Collagen Diagnostic Laboratory at the University of Washington.

REFERENCES

Adzhubei IA, Schmidt S, Peshkin L, Ramensky VE, Gerasimova A, Bork P, Kondrashov AS, Sunyaev SR. 2010. A method and server for predicting damaging missense mutations. Nat Methods 7:248–249.

Baasanjav S, Al-Gazali L, Hashiguchi T, Mizumoto S, Fischer B, Horn D, Seelow D, Ali BR, Aziz SA, Langer R, Saleh AA, Becker C, Nürnberg G, Cantagrel V, Gleeson JG, Gomez D, Michel J-B, Stricker S, Lindner TH, Nürnberg P, Sugahara K, Mundlos S, Hoffmann K. 2011. Faulty initiation of proteoglycan synthesis causes cardiac and joint defects. Am J Hum Genet 89:15–27.

Bernfield M, Götte M, Park P, Reizes O, Fitzgerald ML, Lincecum J, Zako M. 1999. Functions of cell surface heparin sulfate proteoglycans. Annu Rev Biochem 68:729–777.

Bishop JR, Schuksz M, Esko JD. 2007. Heparan sulphate proteoglycans fine-tune mammalian physiology. Nature 446:1030–1037.

Bui C, Huber C, Tuysuz B, Yasemin A, Bole-Feysot C, Leroy JG, Mortier G, Nitschke P, Munnich A, Cormier-Daire V. 2014. XYLT1 mutations in Desbuquois dysplasia type 2. Am J Hum Genet 94:205–414.

Cartault F, Munier P, Jacquemont M-L, Vellayoudom J, Doray B, Payet C, Randiranaivo H, Laville J-M, Munnich A, Cormier-Daire V. 2015. Expanding the clinical spectrum of B4GALT7 deficiency: Homozygous p.R270C mutation with founder effect causes Larsen of Reunion Island syndrome. Eur J Hum Genet 23:49–53.

Faiyaz-Ul-Haque M, Zaidi SHE, Al-Ali M, Al-Mureikhi MS, Kennedy S, Al-Thani G, Tsui L-C, Teebi AS. 2004. A novel missense mutation in the galactosyltransferase-I (B4GALT7) gene in a family exhibiting facioskeletal anomalies and Ehlers–Danlos syndrome resembling the progeroid type. Am J Med Genet Part A 128A:39–45.

Freeze HH. 2006. Genetic defects in the human glycome. Nature Rev 7:537–551.

Guo MH, Stoler J, Lui J, Nilsson O, Bianchi DW, Hirschhorn JN, Dauber A. 2013. Redefining the progeroid form of Ehlers–Danlos syndrome: Report of the fourth patient with B4GALT7 deficiency and review of the literature. Am J Med Genet Part A 161A:2519–2527.

Gulberti S, Lattard V, Fondeur M, Jacquinet J-C, Mulliert G, Netter P, Magdalou J, Ouzzine M, Fournel-Gigleux S. 2005. Phosphorylation and sulfation of oligosaccharide substrates critically influence the activity of human β1,4-galactosyltransferase 7 (GalT-I) and β1,3-glucuronosyltransferase I (GlcAT-I) involved in the biosynthesis of the glycosaminoglycan-protein linkage region of proteoglycans. J Biol Chem 280: 1417–1425.

Häcker U, Nybakken K, Perrimon N. 2005. Heparan sulphate proteoglycans: The sweet side of development. Nat Rev Mol Cell Biol 6:530–541.

Haltiwanger RS, Lowe JB. 2004. Role of glycosylation in development. Annu Rev Biochem 73:491–537.

Kitagawa H, Tone Y, Tamura J-I, Neumann KW, Ogawa T, Oka S, Kawasaki T, Shugahara K. 1998. Molecular cloning and expression of glucuronyltransferase I involved in the biosynthesis of the glycosaminoglycan-protein linkage region of proteoglycans. J Biol Chem 273: 6615–6618.

Kresse H, Rosthøj S, Quentin E, Hollmann J, Glössl J, Okada S, Tønnesen T. 1987. Glycosaminoglycan-free small proteoglycan core protein is secreted by fibroblasts from a patient with a syndrome resembling progeroid. Am J Hum Genet 41:436–453.

Malfait F, Kariminejad A, Van Damme T, Gauche C, Syx D, Merhi-Soussi F, Gulberti S, Symoens S, Vanhauwaert S, Willaert A, Bozorgmehr B, Kariminejad MH, Ebrahimiadib N, Hausser I, Huysseune A, Fournel-Gigleux S, De Paepe A. 2013. Defective initiation of glycosaminoglycan synthesis due to B3GALT6 mutations causes a pleiotropic Ehlers–Danlos syndrome-like connective tissue disorder. Am J Hum Genet 92:935–945.

Nakajima M, Mizumoto S, Miyake N, Kogawa R, Iida A, Ito H, Kitoh H, Hirayama A, Mitsubuchi H, Miyazaki O, Kosaki R, Horikawa R, Lai A, Mendoza-Londono R, Dupuis L, Chitayat D, Howard A, Leal GF, Cavalcanti D, Tsurusaki Y, Saitsu H, Watanabe S, Lausch E, Unger S, Bonafé L, Ohashi H, Superti-Furga A, Matsumoto N, Sugahara K, Nishimura G, Ikegawa S. 2013. Mutations in B3GALT6, which encodes a glycosaminoglycan linker region enzyme, cause a spectrum of skeletal and connective tissue disorders. Am J Hum Genet 92:927–934.

Pönighaus C, Ambrosius M, Casanova JC, Prante C, Kuhn J, Esko JD, Kleesiek K, Götting C. 2007. Human xylosyltransferase II is involved in the biosynthesis of the uniform tetrasaccharide linkage region in chondroitin sulfate and heparan sulfate proteoglycans. J Biol Chem 282:5201–5206.

Schreml J, Durmaz B, Cogulu O, Keupp K, Beleggia F, Pohl E, Milz E, Coker M, Ucar SK, Nürnberg G, Nürnberg P, Kuhn J, Ozkinay F. 2014. The missing "link": An autosomal recessive short stature syndrome caused by a hypofunctional XYLT1 mutation. Hum Genet 133:29–39.

Sugahara K, Mikami T, Uyama T, Mizuguchi S, Nomura K, Kitagawa H. 2003. Recent advances in the structural biology of chondroitin sulfate and dermatan sulfate. Curr Opin Struct Biol 13:612–620.

Von Oettingen JE, Tan W-H, Dauber A. 2014. Skeletal dysplasia, global developmental delay and multiple congenital anomalies in a 5-year-old boy-report of the second family with B3GAT3 mutation and expansion of the phenotype. Am J Med Genet Part A 164A:1580–1586.